Particle Accelerators, 1972, Vol. 3, pp. 35–41 © Gordon and Breach, Science Publishers Ltd. Printed in Glasgow, Scotland

MEASUREMENTS ON SUPERCONDUCTING HELICALLY-LOADED RESONATORS AT HIGH FIELD STRENGTHS

J. L. FRICKE, B. PIOSCZYK AND J. E. VETTER

Institut für Experimentelle Kernphysik, Kernforschungszentrum Karlsruhe, Germany

AND

H. KLEIN

Institut für angewandte Physik, Universität Frankfurt, Germany

A series of measurements on superconducting anodized niobium helices is described. Results for quality factors and maximum obtainable field strengths are presented and breakdown mechanisms are discussed. The best low field Q values at 1.9 °K correspond to a surface resistance of $3.5 \times 10^{-9}\ \Omega$ at a frequency of 90 MHz.

Peak electric fields of 24 MV/m and magnetic fields up to 640 G were measured in short pulse operation. In continuous operation, fields of 17 MV/m and 450 G could be obtained. Field emission increased the losses at high fields.

1. INTRODUCTION

The superconducting helix accelerator research program at this laboratory began in 1969 with the goal of building a pilot accelerator to demonstrate the applicability of rf superconductivity as a preliminary step towards the construction of a larger proton linac which will be used to produce π-mesons.[1] Parameter studies[2] led to a concept in which the proton beam is accelerated from 0.75 MeV to 20 MeV by a series of resonant cavities. These cavities are loaded by half wavelength niobium helices electrically coupled so as to form a structure which is typically $\frac{5}{2}\lambda$ long.

The first series of experiments with superconducting lead and niobium helices was performed in 1970 giving results for the surface resistance as a function of frequency at low power levels, the influence of a static magnetic field[3] and the applicability of dielectric materials.[4] The experimental setup was then converted to a helically-loaded, high-vacuum resonator with a helix of the same geometry as that to be used in the first section of the accelerator. Effects due to coupling of mechanical and electromagnetic forces were then first studied extensively[5] and methods were found for choosing the parameters of the frequency control loop so that stable operation at high field strength was possible.[6]

This paper reports on measurements which were performed to determine the field limitations in a superconducting helix structure with the goal of optimizing the parameters of the pilot accelerator.

No real attempt was made to optimize the surface treatment of the helices used in the present equipment. This remains to be done in future measurements. For the present experiments all methods which have been successful in less complex cavity geometries were adopted, with the exception of the high temperature ultra-high-vacuum treatment[7] which could not be used because of the lack of a suitable furnace.

2. APPARATUS

The geometry of the helically-loaded resonator approximates as closely as possible the first section of the pilot accelerator. This section is operated under the most stringent conditions from the point of view of peak fields and cooling capability as a consequence of the small pitch of the helix at low energies (Table I). For convenience, the shape of the outer conductor was changed with respect to the proposed accelerator design. This has a negligible effect on the helix fields if the separation between the outer conductor and the helix is sufficiently large. Because only a small fraction of the rf losses occur on the outer cylinder, it was fabricated of lead-plated copper in the same way as the proposed accelerator cavities.

TABLE I

Parameters of the helically-loaded resonators

Helix radius	$a = 4.2$ cm
Radius of outer conductor	$b = 12.5$ cm
Pitch	$s = 1.0$ cm
Number of turns	$n = 9$
o.d. of tube	$d = 0.63$ cm
i.d. of tube	$d_i = 0.48$ cm
Resonant frequency	$f_0 = 90$ MHz
Geometry factor	$G = 6.9\,\Omega$

Two kinds of joints between the helix and the outer conductor were tested. In test run ⟨1⟩, to be described below, knife-edge flanges of 40 mm diameter were electron beam welded to the ends of the tube (see Fig. 1). Electrical contact was made by pressing the niobium edges against the lead-plated cover of the resonator. In tests ⟨2a, b, c⟩ the helix ends were electron beam welded to a massive niobium end plate which was then put on the cylindrical part of the resonator (Fig. 2). This method has the advantage that a smaller current density is present at the joint.

Variable probes provided adjustable coupling from coaxial lines to the TM_{01} cut-off mode excited by the E_r field of the helix in two coupling tubes in the top plate of the resonator (Fig. 2). The resonator was evacuated to a vacuum of 10^{-6} torr at room temperature before cooling and then kept below 10^{-6} torr. The earth's magnetic field was shielded to about 5 mOe so that frozen flux would not influence the measurements.[3]

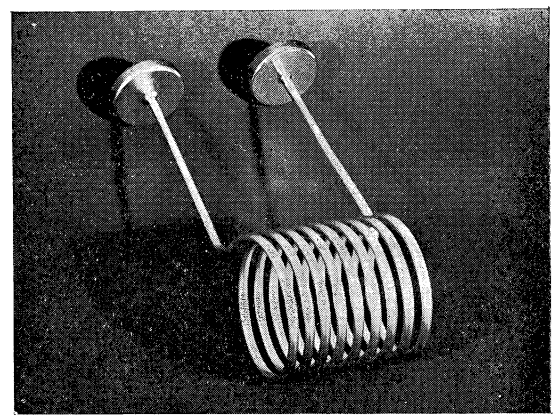

FIG. 1. $\lambda/2$ helix fabricated of niobium with electron beam welded flanges.

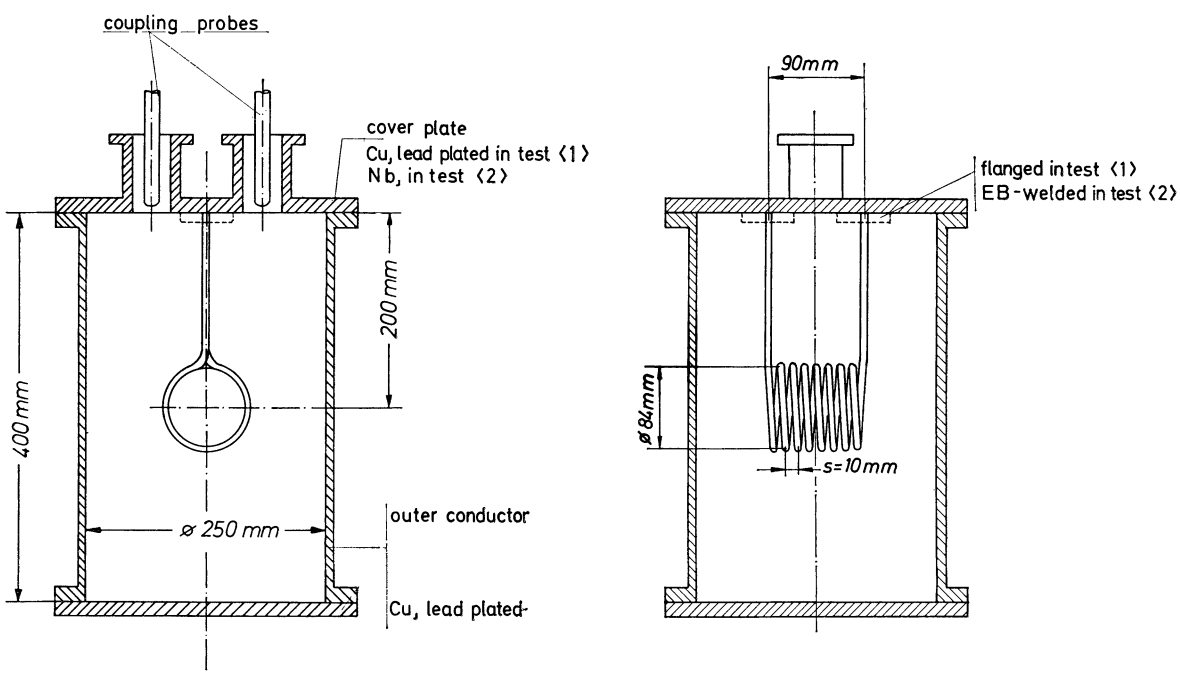

FIG. 2. Cross section of the helically-loaded resonator.

The electrical setup consisted of an rf generator tunable in amplitude and frequency followed by a sequence of amplifiers which provided a maximum power of 50 W. Forward and reflected power were measured at the cavity input line. Q values were determined by recording the decay of the radiated power on a storage oscilloscope after the input line of the resonator was switched from the power amplifier to a 50 Ω load which then terminated the line.

Phase between input and output of the cavity was used to tune the generator frequency.[8] Because of the large static frequency shift at high fields caused by radiation pressure,[5] the narrow band amplifiers and the generator must be tuned to track the resonator frequency. For this reason and because fast power changes favour the excitation of mechanical oscillations of the helix no periodic pulsing of the input power was used.

3. PREPARATION OF THE HELICES

Test ⟨1⟩: The helix was fabricated of $\frac{1}{4}$ in. o.d. niobium tube with a content of less than 500 ppm impurities. The tube was mechanically polished and wound on a mandril. Finally the flanges were electron beam welded to the coil. The surface was further refined by electropolishing ($\sim 35\,\mu$).[9] After this procedure the helix was outgassed for 1 hour at 950 °C at a vacuum of 4×10^{-6} torr to remove hydrogen from the material. Good results with anodized cavities[10] stimulated us to subsequently anodize the helix with a layer of about 300 Å of Nb_2O_5 which gives a golden brownish colour.† The oxide was removed chemically from the flanges to assure good electrical contact to the lead-plated cover.

The preparation procedure for the helix used in tests ⟨2a, b, c⟩ was analogous except that this helix was electron beam welded to a niobium plate which was electropolished and anodized together with the helix. For test ⟨2b⟩, the oxide layer was dissolved and the steps described above, electropolishing, outgassing, and anodizing, were repeated. For test ⟨2c⟩, only the anodized layer was renewed.

† The anodizing was done in a solution of 0.05 per cent H_2SO_4 using a current density of about 0.5 mA/cm².

4. Q-MEASUREMENTS AND AGING EFFECTS

At the beginning of each test the unloaded Q values Q_0 were measured as a function of temperature at lowest power levels. The best Q_0 of 1.9×10^9 at $T<1.9$ °K corresponded to a residual surface resistance of 3.5×10^{-9} Ω at 90 MHz. It might be interesting to note that also with other methods of treatment[3,11,12] no significant better surface resistances could be obtained at VHF until now.

Applying higher power levels to overcome the multipactoring barriers (as discussed below) degraded the Q typically by a factor of 2 or 3. After some days of operation the Q value settled ('aging effect'). Initial Q_0 and aged Q_0's are compiled in Table II.

TABLE II

Quality factor in different test runs. $(Q_0)_{\text{high power}}$ is the Q value measured at a field strength, where increased X-ray level was observed.

Test No.	$(Q_0)_{T<1.7°K}$	$(Q_0)_{T<1.7°K,\text{aged}}$	$(Q_0)_{\text{high power}}$
⟨1⟩	1.7×10^9	9.4×10^8	9×10^7
⟨2a⟩	4.5×10^8	2.6×10^8	10^8
⟨2b⟩	1.7×10^9	6.5×10^8	5×10^8
⟨2c⟩	1.9×10^9	6.5×10^8	9×10^7

Further but reversible decreases of the quality factors were observed with increased field levels as discussed below.

5. DETERMINATION OF FIELD STRENGTHS

The static frequency shift Δf_{stat} of the resonator with power was used as a measure of field strengths after it had been verified that

$$\Delta f_{\text{stat}} \propto P_c Q_0' \propto \omega E^2 \propto \omega B^2.$$

P_c is the power transferred to the cavity corrected for transmission line losses and Q_0' is given by

$$Q_0' = \frac{Q_0 Q_K}{Q_K + Q_0} = (1+\beta) Q_L,$$

Q_0 (the Q value with negligibly small coupling).
Q_L (the Q value at an arbitrary position of the

coupling probes), and the coupling coefficient β are measurable quantities.

Q_K corresponds to the coupling losses.

From Fig. 3, where measured data of both helices are shown, $P_c Q_0'/\mathrm{W} = 1.2 \times 10^5$ $(\Delta f_{\mathrm{stat}}/\mathrm{kHz})$ can be determined.

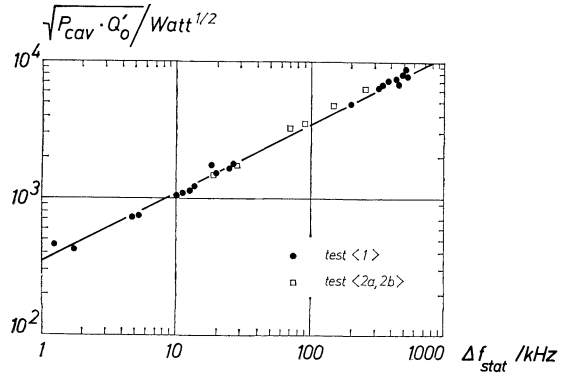

FIG. 3. $(P_{\mathrm{cav}} Q_0)^{1/2}$, a quantity proportional to the peak field, as a function of the static frequency shift, Δf_{stat}.

To relate the easily measurable quantity Δf_{stat} to the field strengths the following procedure was applied:

The fields at the helix surface were calculated by combining the sheath model values[13] with either a ring model[14] or with a model using conformal transformations (CT model).[15] Two corrections were applied to the theoretical values:

Measurements of the axial field of long helices showed that the sheath model fields are systematically higher than the measured values.[16] We corrected for this effect by an 'axial field correction' which, for our helix, lowered all field strengths by about 10 per cent. To take into account the end effects of a short helix comparing perturbation measurements were carried out on a $\lambda/2$ helix and on a long helix with negligible end effects.[16] As a result the calculated field strength values should be multiplied by an 'end field correction factor', which is on the order of 11 per cent.

Axial fields and peaks fields corrected in this way are related to $Q_0' P_c$ and Δf in Table III. Complete agreement was found for the electrical field

TABLE III

Field strength values of ring model and CT model related to measurable quantities $P_c Q_0'$ and Δf_{stat}.

	Ring model	CT model
$E_{0\ \mathrm{axis\ TW}}$	0.13 E	0.13 E
$E_{r\ \max \mathrm{SW}}$	2.0 E	1.92 E
$E_{z\ \max \mathrm{SW}}$	2.0 E	2.0 E
$B_{r\ \max \mathrm{SW}}$	5.34 B	6.95 B
$B_{z\ \max \mathrm{SW}}$	5.24 B	5.26 B

$E = 10^{-3}\ \mathrm{MV/m} \times (P_c Q_0'/\mathrm{W})^{1/2}$
$= 0.346\ \mathrm{MV/m} \times (\Delta f_{\mathrm{stat}}/\mathrm{kHz})^{1/2}$
$B = 10^{-2}\ \mathrm{G} \times (P_c Q_0'/\mathrm{W})^{1/2}$
$= 3.46\mathrm{G} \times (\Delta f_{\mathrm{stat}}/\mathrm{kHz})^{1/2}$

strength calculated with ring and CT models. However, the magnetic peak field values differ by as much as 30 per cent. In the following discussion the CT-model values are given in parenthesis.

6. FIELD DEPENDENT Q AND MULTIPACTORING

Quality factors are plotted as a function of the static frequency for several test runs in Fig. 4. In

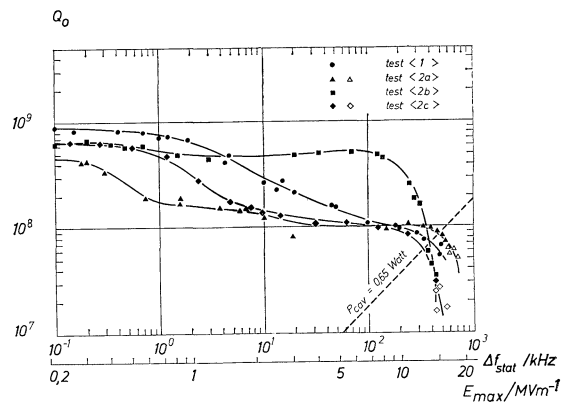

FIG. 4. Q values after 'aging' as a function of the static frequency shift, Δf_{stat}, and of the peak field, $E_{\max}$, for different test runs.

tests $\langle 1 \rangle$, $\langle 2a \rangle$ and $\langle 2c \rangle$ a high field Q of about 10^8 was measured independent of the different low field Q's. As an exception a high field Q of about 5×10^8 was measured in test $\langle 2b \rangle$. This decrease of the quality factor with field strength can hardly be explained by joint effects because the joint configuration was drastically changed from test

⟨1⟩ to ⟨2⟩ and moreover, joint-free, all-niobium, helically-loaded resonators show that same effect.[17] The sharp decrease of the Q values at $\Delta f_{stat} \geqq 300$ kHz was always accompanied by field emission. In this range the quality factors were determined from the relation $\Delta f = 1.2 \times 10^5 \times P_{cav} Q_0'$ taking into account the coupling losses, rather than from decay time measurements.

In all test runs, multipactoring was observed. The corresponding peak field strengths range from 0.3 to 12 MV/m. The fact that the levels are not reproducible from one test run to the other, and even not during one experiment, leads to the assumption that the multipactoring area moved over a geometric range. Surface contamination enhanced the probability of multipactoring: a brief vacuum breakdown into the resonator at helium temperature re-establishes low level multipactoring.

With fast rise pulsing only 'weak' multipactoring barriers can be overcome. A more effective method consists of applying an increased power continuously to the cavity for a longer time ('processing'). During this operation it was observed that the static frequency shift increased linearly with time. Faster rise and an erratic behaviour of Δf_{stat} indicated the end of a multipactoring band. Maintenance at helium temperature and at a vacuum of $< 10^{-6}$ torr was sufficient to prevent further multipactoring.

7. THERMAL BREAKDOWN

Previous studies on heat flow in superfluid helium showed that the heat flow is proportional to the third root of the temperature gradient.[18] An upper limit is given for the heat flow when a temperature of 2.17 °K (λ-point) is exceeded. Recent measurements[19] showed that the maximum transportable heat is limited in tubes of our geometry by boiling if at any cross section of the tube a critical heat flow of 1.7 W/cm^2 is exceeded. As a consequence the helices used in our experiments tolerate a loss of ~ 0.65 W. This thermal breakdown limit is represented as a straight line in Fig. 4. Measured data beyond this line must be explained by losses on the outer conductor. A fast increase of power allows higher peak fields (Table IV) to be obtained. The overload in short time operation differed from one experiment to the other. A maximum increase of the field strengths, a factor of ~ 1.4, was observed in test ⟨2a⟩ for a time of milliseconds.

TABLE IV

Results of maximum obtainable field strengths in several test runs. For each test, the upper values were measured in continuous operation while the lower values were obtained for short term operation. The bracketed values are calculated with the CT model.

Test No.	Δf_{stat} kHz	$E_{0\,TW}$ axis MV/m	$E_{max\,SW}$ MV/m	$B_{max\,SW}$	Dominant mechanism of breakdown
⟨1⟩	550	1.05	16.2	433 (564)	surface
	650	1.15	17.7	470 (685)	losses
⟨2a⟩	600	1.10	17.0	450 (590)	surface
	1200	1.56	24.0	640 (833)	losses
⟨2b⟩	420	0.92	14.2	378 (493)	field
	590	1.09	16.8	450 (584)	emission
⟨2c⟩	445	0.95	14.6	390 (507)	field
	600	1.10	17.0	452 (590)	emission

'Thermal breakdown' and 'magnetic breakdown' show a different picture:

Magnetic breakdown effects as observed in different experimental conditions[20] are characterized by a periodic buildup and breakdown of the cavity field with only negligible time between the two processes. The higher power offered shortens the period time but does not allow higher field strengths to be obtained. In contrast to this behaviour, thermal breakdown allows enhanced field strengths for short periods of time. The breakdown is followed by a comparatively long recovery time of the order of seconds. In this sense, no magnetic breakdown has been observed in our helix experiments.

8. FIELD EMISSION EFFECTS

For $E_{max} \geqq 12$ MV/m an increased X-ray level was observed in a detector outside the dewar. These X-rays are due to field emission electrons which originate from regions of high electric field strength. The best evidence for field emission is a measurement of the X-ray rate as a function of surface field strength E_p.

For field emission, the X-ray rate J is given by[21]:

$$\bar{J} = K_1 \zeta^{2.5} (E_p)^n \phi^{-1} \exp\left(\frac{K_2 \phi^{3/2}}{\zeta E_p}\right),$$

where ζ is the enhancement factor, ϕ the work function and K_1, K_2 are constants, $K_2 = 6.83 \times 10^3$ $\mathrm{MVm^{-1}(eV)^{-3/2}}$, $5 \leqq n \leqq 6.5$ depending on the emission angle of the radiation.

A typical measurement (test ⟨2b⟩) is shown in Fig. 5 in the form of a Fowler–Nordheim plot. Assuming that the electrons are emitted from niobium whiskers, ($\phi = 4$ eV), which penetrated through the oxide layer, enhancement factors

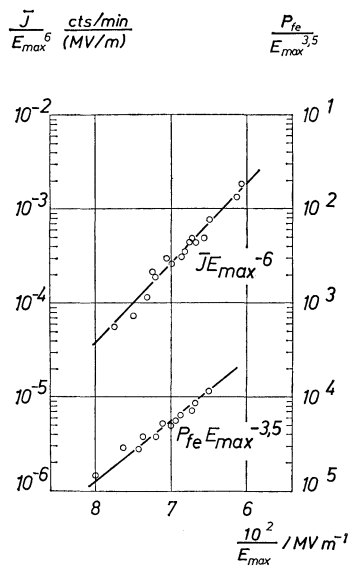

FIG. 5. Fowler–Nordheim plot for the X-ray rate and for the additional losses, P_{fe}, in test ⟨2b⟩.

between 150 and 400 were determined from a variety of measurements at different times during different tests. It was also observed that enhancement factors and the total X-ray intensity for a given field strength changed with time. Our observations showed that long time operation (2 or 3 days) does not necessarily decrease the field emission effect.

If the surface resistance is considered to be constant in the field emission range the surface losses can be separated from the total cavity power loss. The remaining part P_{fe} is also fitted well by a Fowler–Nordheim plot[21] (Fig. 5). This suggests that the increased losses at high fields are only produced by field emission.

In trying to localize field emission in a helically loaded cavity it is useful to make an approximate separation into effects caused by electrons accelerated by the axial fields ('E_z electrons') and radial fields ('E_r electrons'). This separation is useful for two reasons.

First, the spatial distribution and energy of X-rays on the outside will be different for E_z and E_r electrons. E_z electrons are primarily accelerated from coil to coil and are expected to produce an approximately homogeneous spatial distribution. E_r electrons are accelerated from the helix to the wall and are expected to produce an intensity maximum in a plane perpendicular to the helix axis (see Fig. 6). Since the potential difference

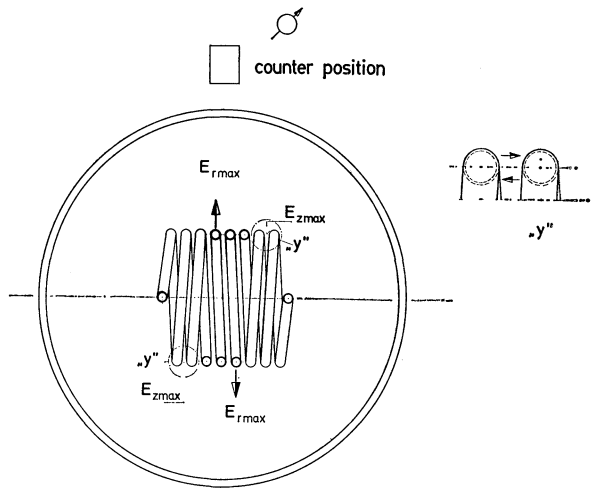

FIG. 6. Cross section of the helically-loaded resonator. Paths of field emission electrons in E_{zmax} and E_{rmax} areas are indicated.

along the path is greater for E_r electrons, they are expected to have a higher energy.

Second, the effect of E_z and E_r electrons on the cavity is different. E_z electrons dissipate their energy in the helix and contribute directly to the heat which must be transported by the superfluid helium.

E_r electrons, on the other hand, do not contribute to this heat load but only to the general power loss of the entire cavity.

As a consequence, in tests ⟨2b⟩ and ⟨2c⟩, stable operation could be maintained at cavity powers exceeding by far the breakdown limit of the helix (see Fig. 4).

In order to localize the source of field emission, we measured the energy spectra of the bremsstrahlung at different positions outside the dewar. For test ⟨2a⟩, at a lower field level of $E_{max} \simeq 14$ MV/m, the X-ray rate was nearly independent of detector position (E_z electrons). However for $E_{max} \geqq 16$ MV/m an intensity maximum was observed perpendicular to the helix axis. The spectrum at this position contained radiation of higher energy (E_r electrons).

These observations lead to the assumption that in this experiment $E_{zmax} > E_{rmax}$ since the field emission limit is reached for E_z first. This is in contrast to calculations described above which predict approximately equal values of E_{zmax} and E_{rmax}. It can further be stated that at higher field levels E_{zmax} and E_{rmax} areas emit electrons simultaneously.

One conclusion which may be drawn from these observations is that early thermal breakdown due to field emission may be avoided by choosing the helix parameters so that E_{zmax} is sufficiently smaller than E_{rmax}.

9. CONCLUSIONS

With electropolished and anodized helices, fabricated of niobium, peak electric fields of about 17 MV/m could be obtained in steady-state operation.

Only thermal breakdown was observed. This was caused in some experiments by field emission and in others by excessive surface resistance.

Applying the maximum field strength result to the problem of calculating the accelerating component of the field on the axis of a long helix (or a coupled helix chain), an accelerating field component of about 1.5 MV/m may be obtained at a phase velocity of 0.04 c, i.e. at the beginning of the accelerator.

Breakdown limits due to peak fields and power loss can now be used to optimize the parameters of the proposed super-conducting helix accelerator.

ACKNOWLEDGEMENTS

This work was performed with the support and encouragement of Prof. A. Citron and Dr. M. Kuntze. Discussions with members of the linac group are thankfully acknowledged. G. Merz has made valuable contributions in model measurements and O. Siart in calculation of peak fields. The rf-feedback circuit was built with the help of H. Strube and D. Schulze. The electropolishing and anodizing was made with the aid of P. Kneisel. The authors are grateful to N. Münch and G. Westenfelder for help in the construction and operation of the apparatus.

REFERENCES

1. A. Citron, *Proc. 1970 Proton Linear Accelerator Conference, National Accelerator Laboratory, Batavia, Ill.*, **1**, 239.
2. H. Klein and O. Siart, *ibid.*, 293.
3. J. E. Vetter *et al.*, *ibid.*, 249.
4. K. Mittag *et al.*, *ibid.*, 257.
5. D. Schulze, *ibid.*, 359.
6. D. Schulze *et al.*, *IEEE Trans. Nucl. Sci.*, **NS-18, 3**, 160 (1971).
7. J. P. Turneaure and Nguyen Tuong Viet, *Appl. Phys. Letters*, **16**, 333 (1970).
8. H. Strube, Ges. f. Kernforschung Karlsruhe, to be published.
9. H. Diepers *et al.*, Siemens Erlangen, to be published in *Phys. Letters.*
10. H. Martens *et al.*, *Phys. Letters*, **34A**, 439 (1971).
11. H. F. Glavish *et al.*, Proposal to the National Science Foundation, High Energy Physics Laboratory, Stanford University (1971).
12. P. H. Ceperley, Stanford University Report HEPL 655 (1971).
13. K. Johnson, Chr. Michelsens Inst., *Beretn.* **14** and **16**, (1951), (1954).
14. O. Siart, Dissertation Universität Frankfurt (1970).
15. A. Sierk *et al.*, *Particle Accelerators*, **2**, 149 (1971).
16. O. Siart *et al.*, to be submitted to *Particle Accelerators.*
17. Private communication, High Energy Physics Laboratory, Stanford University.
18. P. R. Critchlow and R. A. Hemstreet, *J. Appl. Phys.* **40**, 2675 (1969).
19. G. Krafft, Kernforschungszentrum Karlsruhe, to be published.
20. G. Dammertz *et al.*, *IEEE Trans. Nucl. Sci.* **NS-18, 3**, 153 (1971).
21. H. Schopper *et al.*, Ext. Report 3/68-6, Kernsforschungszentrum Karlsruhe (1968).

Received 9 September 1971